

## THIN-SKIN ELECTROMAGNETIC FIELDS AROUND SURFACE-BREAKING CRACKS IN METALS

A.M. Lewis, D.H. Michael, M.C. Lugg and R. Collins

Wolfson NDE Unit  
Department of Mechanical Engineering  
University College London  
Torrington Place, London, WC1E 7JE, UK

### INTRODUCTION

In situations where the electrical skin depth  $\delta$  is small compared with a typical crack dimension  $l$ , substantial progress has been achieved in recent years in modeling surface electromagnetic fields and the perturbations that are produced in them by surface-breaking flaws [1,2,3]. The development of an unfolding theory at UCL for thin-skin surface fields was based on the approximation that the electric and magnetic field vectors  $\mathbf{E}$  and  $\mathbf{H}$  are essentially tangential to the surface of the material in the surface skin. It was motivated by the desire to measure fatigue cracks in ferrous materials used in large-scale steel structures such as offshore oil rigs [2], and the method to which it was applied was the a.c. field measurement technique. Auld et al [4,5] later adapted the unfolding approach in considering thin-skin field models for the eddy current method, and their major concern was with applications to non-ferrous materials used in airframe and aero-engine manufacture. For acfm work, the unfolding theory leads to a surface Laplacian field on both the metal surface and the crack face and information on the crack presence is deduced by measuring perturbations in the surface field. Auld's model for eddy currents also has a plane Laplacian field on the crack face, but it is assumed that the crack produces no change in the field on the metal surface. Field lines in the unfolded plane for both models are shown schematically in Figure 1(b,c) for the case when the interrogating field is uniform and the crack is semi-circular. Auld's model has been described as a Born type of approximation from an analogy with wave scattering theory which ignores the scattered field when calculating scattering cross-sections.

It has been puzzling for some time that these two apparently disparate approaches have both given good agreement with experiment in their respective areas of application. This paper outlines recent work [6,7] which shows that the key to reconciling these two models rests in understanding how the electromagnetic field outside the specimen couples with the surface field. The contrasting boundary conditions which are imposed on the magnetic scalar potential at the metal surface in these two models are found to be two extremes of a more general condition and they are linked by the important dimensionless parameter  $m = l/\mu_r\delta$  where  $\mu_r$  is the relative permeability of the material. The surface Laplace limit appropriate to the acfm work is recovered as  $m \rightarrow 0$ , whereas the Born limit is appropriate as  $m \rightarrow \infty$ .

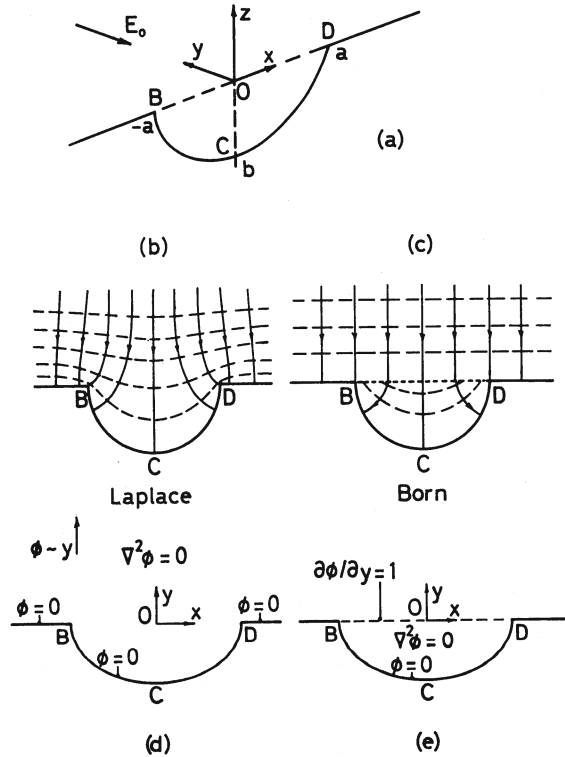


Figure 1. (a) Geometry for the problem of a semi-elliptical crack interrogated by a uniform incident surface current.  
 (b,c) Schematic field lines from surface Laplace and Born models for a semi-circular crack.  
 (d) The unfolded problem for the surface electric potential  $\phi$  for a semi-elliptical crack in the Laplacian limit.  
 (e) The boundary value problem on a semi-elliptical crack face in the Born limit.

## FORMULATION

Cartesian axes oriented as shown in Figure 1(a) are used, the conductivity  $\sigma$ , permeability  $\mu$  and dielectric constant for the material are considered constant, the free space permeability is  $\mu_0$  and the time dependence is like  $\exp(i\omega t)$ . The frequencies considered are too low for radiation effects to be important so that the Maxwell equations for the fields in the exterior are

$$\text{curl}\mathbf{E} = -i\omega\mu_0\mathbf{H}, \quad \text{div}\mathbf{E} = 0, \quad \text{curl}\mathbf{H} = 0, \quad \text{div}\mathbf{H} = 0 \quad (1,2,3,4)$$

and in the skin

$$\text{curl}\mathbf{E} = -i\omega\mu\mathbf{H}, \quad \text{div}\mathbf{E} = 0, \quad \text{curl}\mathbf{H} = \sigma\mathbf{E}, \quad \text{div}\mathbf{H} = 0 \quad (5,6,7,8)$$

We work with a magnetic scalar potential  $\psi$  where  $\mathbf{H} = \text{grad } \psi$  so that in the exterior we have

$$\frac{\partial^2\psi}{\partial x^2} + \frac{\partial^2\psi}{\partial y^2} + \frac{\partial^2\psi}{\partial z^2} = 0 \quad (9)$$

It follows from (5) to (8) that in the conductor

$$\frac{\partial^2\mathbf{E}}{\partial x^2} + \frac{\partial^2\mathbf{E}}{\partial y^2} + \frac{\partial^2\mathbf{E}}{\partial z^2} = k^2\mathbf{E}, \quad \frac{\partial^2\mathbf{H}}{\partial x^2} + \frac{\partial^2\mathbf{H}}{\partial y^2} + \frac{\partial^2\mathbf{H}}{\partial z^2} = k^2\mathbf{H} \quad (10,11)$$

where  $k^2 = i\omega\sigma\mu$  ( $\text{Re } k > 0$ ). The skin depth  $\delta$  is measured by the length  $1/|k|$ ; we are concerned with thin-skin fields for which  $\delta/l \ll 1$ ,  $l$  being the length scale of the surface-breaking crack of finite aspect ratio. Perturbations in  $\mathbf{E}$  and  $\mathbf{H}$  produced by the crack in the exterior field occur on the length scale  $l$  in the  $x, y, z$  directions. In the surface skin, however, while the  $x$  and  $y$  dependence occurs on the same length scale  $l$ , in the  $z$  direction changes occur on the much smaller length scale  $\delta$ . It follows from (10) and (11) that  $|\partial^2/\partial x^2|$  and  $|\partial^2/\partial y^2|$  are both  $\ll |\partial^2/\partial z^2|$  so that the skin profiles for the  $\mathbf{E}$  and  $\mathbf{H}$  fields must be like  $\exp(kz)$  to a high degree of approximation. We are concerned here with a closer examination of the balance between the various terms in (10) and (11). The interior and exterior fields must obey the boundary conditions that tangential components of  $\mathbf{H}$  and the normal components of  $\mathbf{B} = \mu\mathbf{H}$  are continuous at their interface  $z = 0$ . Thus the  $\mathbf{H}$  field in the skin may be written

$$H_x \sim \left(\frac{\partial\psi}{\partial x}\right)_0 e^{kz}, \quad H_y \sim \left(\frac{\partial\psi}{\partial y}\right)_0 e^{kz}, \quad H_z \sim \frac{\mu_0}{\mu} \left(\frac{\partial\psi}{\partial z}\right)_0 e^{kz} \quad (12)$$

where the suffix 0 applied to the derivative denotes evaluation at the metal surface. From (8) therefore

$$\left[ \left(\frac{\partial^2\psi}{\partial x^2}\right)_0 + \left(\frac{\partial^2\psi}{\partial y^2}\right)_0 + \frac{k\mu_0}{\mu} \left(\frac{\partial\psi}{\partial z}\right)_0 \right] e^{kz} = 0 \quad (13)$$

so that a boundary condition on  $\psi(x, y, z)$  at the metal surface  $z = 0$  is

$$\frac{\partial^2\psi}{\partial x^2} + \frac{\partial^2\psi}{\partial y^2} + \frac{k\mu_0}{\mu} \frac{\partial\psi}{\partial z} = 0 \quad (14)$$

A similar derivation also applies for materials of high dielectric constant [8]. From (7)

and (12), corresponding values of the components of  $\mathbf{E}$  in the surface may be shown [6] to be

$$E_x \sim \frac{-k}{\sigma} \left( \frac{\partial \Psi}{\partial y} \right)_0 e^{kz}, \dots, E_y \sim \frac{+k}{\sigma} \left( \frac{\partial \Psi}{\partial x} \right)_0 e^{kz}, \dots, E_z \sim 0 \quad (15)$$

Now the scaling of the last term in (14) relative to the first two is given by the dimensionless parameter

$$m = l/\mu_s \delta \quad (16)$$

and it is the value of this parameter which accounts for the difference between the two models of surface fields described above. For ferrous steels at relatively low frequencies,  $m$  is small and the limiting form of equation (14) is the plane Laplacian condition

$$\frac{\partial^2 \Psi}{\partial x^2} + \frac{\partial^2 \Psi}{\partial y^2} = 0 \text{ at } z = 0 \quad (17)$$

This limit then produces the plane Laplacian unfolding model. For non-magnetic materials like aluminum where  $\mu_r=1$ , however,  $m$  is necessarily large in thin-skin situations and the limiting form of equation (14) then requires

$$\frac{\partial \Psi}{\partial z} = 0 \text{ at } z = 0 \quad (18)$$

This is the surface condition underlying the Born approximation used by Auld et al [4,5], in which the image of the interrogating field is applied to remove the normal component of  $\mathbf{H}$  at  $z = 0$  and no other back scattering terms are used on the surface. The parameter  $m$ , through its influence on the general boundary condition (14), thus reconciles the two models described in the Introduction. The plane Laplace limit is recovered when  $m \rightarrow 0$ , the Born limit arises as  $m \rightarrow \infty$ ; it seems inappropriate now to refer to the latter as an approximation in this context, since it is correct at the appropriate limit. The authors have undertaken theoretical and experimental investigations to confirm these two limiting forms of solution when  $m \rightarrow 0$  and  $m \rightarrow \infty$  in the case in which a surface crack of semi-elliptical plan form is interrogated by a uniform current injected into the specimen. The experiments confirm that the field adjacent to the crack takes up the form expected from the unfolding model for small  $m$  and the Born model for large  $m$ .

## THE MAGNETIC FIELD ABOVE A FLAW

We consider the problem of a semi-elliptical crack interrogated with a uniform incident current as in Figure 1(a). The major and minor semi-axes are denoted by  $a$  and  $b$ . The solution of equation (9) for the scalar magnetic potential  $\psi$  subject to the boundary condition in equation (14) has been obtained for the two limits  $m \rightarrow 0$  and  $m \rightarrow \infty$  by Fourier transform methods [6]. Construction of these solutions requires a preliminary consideration of the non-analytic behavior of the fields at the edge of the crack. As a consequence of the symmetry of the fields about the crack plane, OBCD, we note first that  $\psi$  and hence  $\partial\psi/\partial x$  are continuous functions across the crack from one edge to the other. However,  $H_y$  or  $\partial\psi/\partial y$  is discontinuous across the crack edge  $|x| < a$ ,  $y = x = 0$ , but  $H_y = 0$  for  $|x| > a$ ,  $y = z = 0$ . A second effect of the crack is to produce a flux of  $H_z$  out of the crack edge per unit length. We can incorporate these two features into the surface condition (14) and show that [6]

$$\frac{\partial^2 \Psi}{\partial x^2} + \frac{\partial^2 \Psi}{\partial y^2} + \frac{k\mu_0}{\mu} \frac{\partial \Psi}{\partial z} = 2H_{z0}(x)\delta(y) \quad (19)$$

where  $\delta(y)$  is the Dirac delta function and  $H_{z_0}(x)$  represents the  $z$  component of  $\mathbf{H}$  on the crack face at the edge. If equation (19) is multiplied throughout by  $\mu/k$  it can be seen as an equation of conservation of the flux of  $\mathbf{B}$  in the surface layer at  $z = 0$ . On the LHS the first two terms together represent the flux of  $\mathbf{B}$  per unit area out of an area in the  $(xy)$  plane within the layer. Outside the crack this is balanced by the flux of  $\mathbf{B}$  entering the layer from outside, represented by the third term on the LHS. The terms on the RHS represent the sources of flux arising at the crack mouth. These sources of magnetic flux are provided by the flux of  $\mathbf{B}$  into the surface  $z = 0$  from the two crack faces.

Equation (19) demonstrates the way in which the magnetic flux out of the crack is directed in the two limiting cases. In the limit when  $m$  is small the equation becomes

$$\frac{\partial^2 \psi}{\partial x^2} + \frac{\partial^2 \psi}{\partial y^2} = 2H_{z_0}(x)\delta(y) \quad (20)$$

which shows that all the magnetic flux emerging from the crack is directed into the surface plane. When  $m$  is large the equation becomes

$$\frac{k\mu_0}{\mu} \frac{\partial \psi}{\partial z} = 2H_{z_0}(x)\delta(y) \quad (21)$$

which signifies that all the flux is directed into the space  $z > 0$ . These limiting cases are illustrated schematically in Figure 2 and they enable us to specify the boundary conditions which must apply when joining the fields on the crack face and the surface plane. Irrespective of the value of  $m$  we must ensure that the normal flow of current across the crack edge is conserved. Since the skin profiles are the same in both regions it follows that the normal  $\mathbf{E}$  component,  $E_n$  must be continuous at the edge where, in addition to this, the joining condition (19) must also apply. In the Laplacian limit shown in Figure 2(a) the flux of  $\mathbf{B}$  emerging from the crack face is wholly directed into the plane. Since  $\mathbf{E} = 0$  in the interior at the point  $i$ , then the component of  $\mathbf{E}$  on the surfaces tangential to the crack edge is a measure of this flux and it follows that  $E_t$  has the same value at the points  $p, q$ .  $E_t$  is therefore continuous across the edge. These two conditions, the continuity of  $E_t$  and  $E_n$ , have been the basis of all previous modeling of the surface fields in the Laplacian limit. In the Born limit shown in figure 2b, since all the flux emerging from the crack is directed across the corner into the free space, a change in  $E_t$  from one side of the crack edge to the other arises. In the cases where the applied field is symmetrical about the crack plane, no flux of  $\mathbf{B}$  occurs across this plane. It follows that on the outer edge at  $p$ ,  $E_t$  is the same as in the interior of the specimen i.e.  $E_t = 0$ . This is the case in the problem considered in this paper where the crack is interrogated by a uniform incident current. The Born condition,  $\partial\psi/\partial z = 0$  outside the crack at  $z = 0$ , is satisfied in this case by the uniform current flow remaining unchanged so that  $E_x = E_t$  is everywhere zero on the surface plane.

It should be noted that this discussion of the edge conditions does not take account of the corner transition between the two planes which takes place on a length scale  $\delta$  at the corner. The solutions there for the Laplacian limit were given by Michael et al [9]. The surface boundary condition on  $\psi$  in equation (14) appears also in papers by Senior [8] and Nicolas [10], but they are not concerned with crack measurement and detection and they do not proceed to the deductions and interpretations outlined above.

The field problems posed in the two limits  $m \rightarrow 0$  and  $m \rightarrow \infty$  are set out in Figure 1(d,e) in terms of the potential  $\phi$  for the surface  $\mathbf{E}$  field. Formulation in terms of  $\phi$  was adopted because the solution for the limit  $m \rightarrow 0$  already existed in those terms [11]. The solution for the limit  $m \rightarrow \infty$  in the domain of the crack face OBCD has been obtained by Fourier analysis [6]. The value of  $H_{z_0}$  at the crack edge is then obtained from these solutions by evaluating  $\partial\phi/\partial x$  along the crack surface edge BOD.

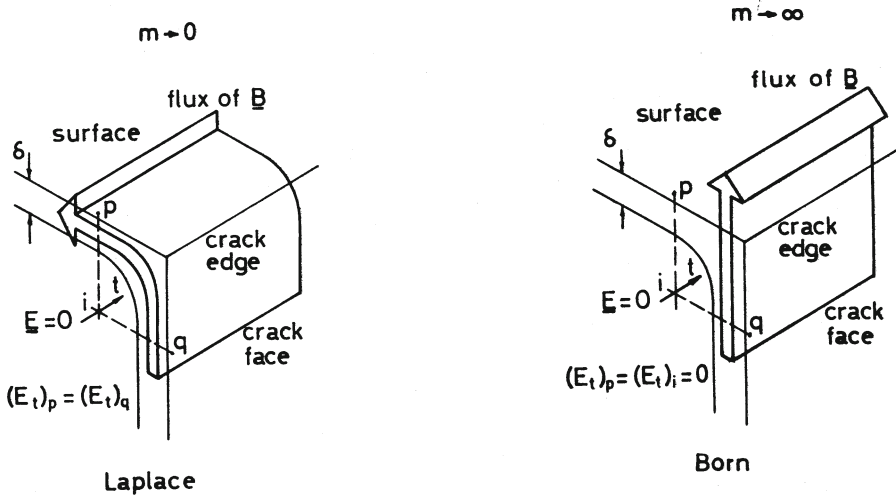


Figure 2. The flux of  $B$  in the Laplace and Born limits.

In the Born limit, the mouth of the crack acts as a strong source of magnetic flux into the space  $z > 0$  so that the magnetic field there is much more sensitive to the mouth opening than it is for the Laplacian limit. For small openings, a correction for the effect can be calculated in the Born limit. The model assumes a constant tangential  $H$  field across the gap between opposite faces of the crack. At the mouth of the crack we can therefore calculate the correction to the flux of  $B_z$  assuming that  $B_z$  is constant across the mouth. Thus if  $h$  represents the mouth opening, which we here assume to be a constant independent of  $x$ , the total flux of  $B_z$  from the crack is changed to  $H_{z0} \{2\mu/k + \mu_0 h\}$  where  $h \ll l$ . The ratio of the magnitudes of the two terms in the bracket is seen to be  $mh/2l$ , which illustrates why the Born model is sensitive to this effect since  $m \gg 1$  in this case. The effect of this additional term was included when calculating the numerical results for the Born model. The results of the numerical calculations are presented as graphs of  $B_z/B_0$  where  $B_0$  is the unperturbed magnitude of  $B$  upstream of the crack.

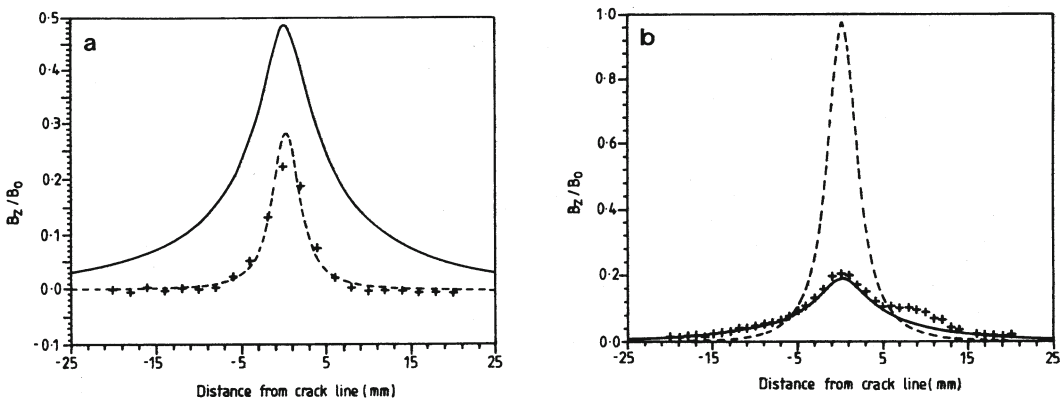


Figure 3. Comparison of experimental values of  $B_z/B_0$  for a scan at a height of 2 mm across a semi-elliptical crack, with the theoretical estimates from the Laplacian and Born limits, (a) for a fatigue crack of half-length  $a = 18.5$  mm and depth  $b = 3.0$  mm in mild steel, scanned 4.5 mm in from an end, (b) for a notch of  $a = b = 20$  mm in Dural NS8 aluminum alloy, scanned across an end.  
 + Experimental results, — Laplacian theory, - - - - Born theory.



## EXPERIMENTAL CONFIRMATION

Experiments were carried out on a plate of mild steel containing a surface-breaking fatigue crack of semi-elliptical form and an aluminum block into which a semi-elliptical spark-eroded notch had been machined. The values of the parameter  $m$  were 0.59 in the former case and 11.9 in the latter thus reproducing the low  $m$  and high  $m$  limits respectively. Magnetic field strengths  $B_x$ ,  $B_y$ ,  $B_z$  were measured with small coils, the induced voltages being measured on a conventional acfm instrument, the Crack Microgauge. A uniform incident field was established by direct injection into the ends of the blocks. The surfaces were scanned by the coils which were mounted on a motorized x-y table.

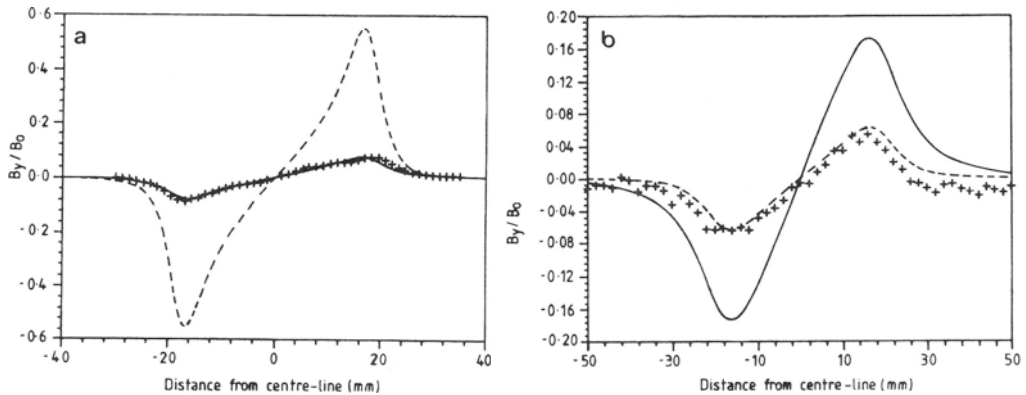


Figure 4. Comparison of experimental values of  $B_y/B_0$  for a scan at a height of 2 mm parallel to the edge of a semi-elliptical crack, with the theoretical estimates from the Laplacian and Born limits, (a) for the same fatigue crack in mild steel at a distance of 3 mm from the crack edge, (b) for the same notch in Dural NS8 at a distance of 7 mm from the crack edge.  
 + Experimental results, — Laplacian theory, - - - - Born theory.

Figure 3 shows a comparison of the experimental values of  $B_x$  with the theoretical predictions of both models for a traverse in the  $y$  direction across the crack near one end. The experimental points in this case represent an average over the two ends. The results clearly confirm the conclusions of our theory that the results for steel should agree with the Laplacian model, whilst those for aluminum should follow the Born model. In fact the agreement in the steel experiments is better than might be expected because the value of  $m$  is not very small in this experiment. These figures also demonstrate one of the main differences between the models, namely that the  $B_x$  field is much more strongly concentrated over the crack edge in the Born model. Further confirmation of the modeling comes from the results shown in Figure 4 in which  $B_y$  is plotted for a traverse in the  $x$  direction i.e. parallel to the crack edge. This is a particularly useful component of  $\mathbf{B}$  to measure because the anti-symmetry of  $B_y$  with  $y$  allows much of the non-uniformity of the field to be eliminated by averaging. In each case the appropriate model happens to be the one which gives the smaller values of  $B_x$ . We note finally that in these experiments the crack opening in the steel specimen is very small and has negligible effect. On the other hand for the aluminum spark eroded notch  $h = 0.8\text{mm}$  and the value of  $mh/2a$ , which measures the relative contribution of the crack opening to the  $B_x$  flux is in this case 0.236.

## CONCLUSIONS

From a general model which matches the thin-skin electromagnetic field around a surface breaking crack to that in the free space above, we have found that the solution has two extremes, depending on the value of the ratio  $m = l/\mu_r\delta$  where  $l$  is the length scale of the crack. For  $\mu_r \gg 1$  the magnetic scalar potential satisfies the 2-D Laplace equation on the surface, which explains why this approximation, used in modeling the a.c.f.m. technique, gives good results for magnetic materials such as mild steel. For the opposite extreme, where  $\mu_r \sim 1$ , the scalar potential satisfies the condition that its normal derivative is zero, which explains why the Born approximation, often used in modeling the eddy current technique, gives good results for non-magnetic materials such as aluminum. It has also been shown that the results are sensitive to the notch opening when  $m$  is large. Experiments undertaken to measure the magnetic field above cracks subjected to a uniform input current have given good quantitative agreement with the theoretical predictions. Further work is in progress to determine what ranges of  $m$  can be described by each extreme, and to solve the general problem for intermediate  $m$ .

## ACKNOWLEDGEMENT

This work was funded by an award from the Wolfson Foundation. The authors are also grateful for discussions with Prof. B.A. Auld who visited the Mathematics Department at University College London, with support from SERC Grant GR/E/07180.

## REFERENCES

1. W.D. Dover, F.D.W. Charlesworth, K.A. Taylor, R. Collins and D.H. Michael in "Eddy Current Characterisation of Materials and Structures" (G. Birnbaum and G. Free, eds.), ASTM, Philadelphia pp 401-427, (1981).
2. R. Collins, W.D. Dover and D.H. Michael in "Research Techniques in Non-Destructive Testing" Vol. 8 (R.S. Sharpe, ed.), Academic Press, London, UK pp 211-267, (1985).
3. R. Collins and D.H. Michael in "Mathematical Modeling in Non-Destructive testing" (M. Blakemore and G. Georgiou, eds.), O.U.P. pp 279-298, (1988).
4. B.A. Auld, F. Muenneman and M. Riazat in "Research Techniques in Non-Destructive Testing", Vol 7 (R.S. Sharpe, ed.), Academic Press, London, UK pp 37-76, (1984).
5. B.A. Auld, S. Jefferies, J.C. Moulder and J.C. Gerlitz in "Review of Progress in Quantitative Non-Destructive Evaluation", 5 (D.O. Thompson and D.E. Chimenti, eds), Plenum Press, New York pp 383-393, (1986)
6. A.M. Lewis, D.H. Michael, M.C. Lugg & R. Collins, J. App Phys. (in the press)
7. M.C. Lugg, A.M. Lewis, D.H. Michael & R. Collins in "Electromagnetic Testing", IOP Short Meetings no 12, Institute of Physics, Bristol (1988).
8. T.B.A. Senior, Appl.Sci.Res. B 8, pp 418-436, (1960).
9. D.H. Michael, R.T. Waechter and R. Collins, Proc. Roy. Soc. A 381, pp 139-157, (1982).
10. A. Nicolas, IEEE Transactions on Magnetics, 24 pp 130-133 (1988).
11. R. Collins, D.H. Michael and K.B. Ranger, Proc. of 13th Symp. on Non-Destructive Evaluation (B.E. Leonard, ed.) Nondestructive Testing Information Analysis Center at South-West Research Institute, San Antonio, Texas, pp 470-479, (1981).